MJFAS
Malaysian Journal of Fundamental and Applied Sciences

Pratiwi *et al.* | Malaysian Journal of Fundamental and Applied Sciences, Vol. 22 (2026) 90–101

RESEARCH ARTICLE

Identification of Subsurface Geological Structures of the Arjuno-Welirang Geothermal Potential Area Using the Gravity Method

Ratih Nur Jaya Pratiwi[a,b]*, Agustya Adi Martha[c], Hartono[b], Rizki Wijayanti[b], Ahmad Ali Muckharom[d], Amelia Siffa Arum Kinanti[b], Nanda Putri Nurul Ngaeni[b].

[a]PT Pro Tech Engineering, Tambun Utara, Bekasi 17510, West Java, Indonesia; [b]Department of Physics, Faculty of Mathematics and Natural Sciences, Jenderal Soedirman University, Purwokerto 53122, Central Java, Indonesia; [c]Limnology and water resource research center, BRIN RI, Cibinong, Bogor 16911, West Java, Indonesia; [d]Department of Physics, Faculty of Science and Mathematics, Diponegoro University, Tembalang, Semarang 50275, Central Java, Indonesia

Abstract Java Island has several geothermal prospects, one of which is located in the Arjuno–Welirang area in East Java. The objective of this study is to determine the subsurface geological structures that have the potential to generate geothermal energy in the region. The study utilizes a gravity-based method that is based on the Global Gravity Model Plus. Complete Bouguer anomalies, first horizontal derivative, and second vertical derivative were analyzed to identify fault structures. Additionally, 2D modeling was performed using inversion modeling implemented in the ZondGM2D software. A total of six major faults were identified four normal faults and two reverse faults primarily distributed near active geothermal manifestations such as Padusan hot springs, Coban Hot Springs and Mount Welirang. Furthermore, 2D gravity inversion modeling was performed along two main profiles (A–A′ and B–B′). The inversion results revealed three key subsurface layers: (1) a low-density zone (<2.3 g/cm³) interpreted as a clay cap formed by hydrothermal alteration, (2) an intermediate-density reservoir zone (2.3–2.5 g/cm³) composed of fractured volcanic rocks, and (3) a high-density magmatic intrusion zone (>2.6 g/cm³) serving as the heat source.

Keywords: Geothermal, Derivative Analysis, 2D Modeling, Inversion.

Introduction

***For correspondence:**
ratihnurjayapratiwi@gmail.com

Received: 30 June 2025
Accepted: 31 Dec. 2025

Geothermal energy is a renewable energy source with great potential to support the fulfillment of national energy needs in the future [1]. Compared to fossil fuels, geothermal power plants are more sustainable and environmentally friendly [2]. The growing energy demand driven by population growth and industrialization, along with the environmental and health impacts of fossil fuel consumption, has increased the urgency to transition toward clean and sustainable energy sources. As a renewable resource capable of providing continuous and reliable energy, geothermal energy offers a viable pathway to replace fossil fuels while enhancing national energy security [3].

Efficient subsurface exploration methods are needed to optimize geothermal energy utilization and identify the characteristics of geothermal systems [4]. Identifying and mapping subsurface geological structures are critical steps in exploring geothermal potential, particularly in understanding the geological controls on geothermal system components. An effective geophysical method that supports this study is satellite-based gravity methods. The gravity method is utilized to detect subsurface structural features, including stratigraphic layering and fluid pathways, which correspond to recharge and discharge zones

within geothermal systems. The fundamental principle underlying this method is the variation in rock density, where thermal sources and subsurface heat accumulation zones generate measurable density contrasts relative to the surrounding geological materials [5]. Based on this principle, low density gravity anomalies are commonly interpreted as geothermal reservoirs or hydrothermally altered zones, whereas high density anomalies are associated with intrusive or molten bodies acting as geothermal heat sources [6]. In this study, gravity data derived from the Global Gravity Model Plus (GGMplus) are utilized to capture these density variations. Previous studies have demonstrated that a comparison between GGMplus gravity disturbance data and terrestrial Bouguer gravity measurements shows a high correlation, indicating that satellite derived gravity data can represent subsurface density variations consistently with field observations [7]. In Indonesia, researchers have utilized GGMplus data to identify active faults [8], assess liquefaction potential [9], delineate hydrocarbon accumulations [10] and evaluate geothermal potential [11]. The gravity modeling results from these studies show good similarity with geological information, seismicity data, as well as resistivity and magnetotelluric survey results. As a result, this method is cost and time efficient, as it reduces the need for extensive direct field surveys without compromising data accuracy. Satellite based gravity imagery provides sufficient density contrast to identify subsurface anomalies, playing a crucial role in assessing the geothermal system potential [12].

Java Island has eleven geothermal prospects, accounting for about 5% of the national total [13]. One of these prospects is located in the Arjuno-Welirang area in East Java [12]. The Arjuno-Welirang area consists of two stratovolcanoes: Mount Arjuno, which reaches 3,339 meters above sea level, and Mount Welirang, which reaches 3,156 meters. The area has been designated a Geothermal Working Area since 2017, with an estimated potential of 200 MW. PT Geo Dipa Energi has an initial development plan of 150 MW. Hot springs and fumaroles at the summit of Mount Welirang indicate the presence of an active geothermal system [14]. In this context, gravity methods are used to identify subsurface geological structures and map the distribution of rock density associated with the geothermal system in the Arjuno-Welirang area.

Regional Geology of the Arjuno-Welirang Area

The Arjuno-Welirang area is located in the administrative regions of the Malang and Mojokerto Regencies. The area's geology is dominated by Quaternary volcanic rocks, indicating relatively recent volcanic activity and the potential for geothermal energy generation [15]. An important aspect of geothermal system studies is understanding the regional geological and stratigraphic conditions, which describe an area's volcanic history and geodynamic evolution. Figure 1 shows the regional stratigraphy of the Arjuno-Welirang Volcanic Area and its surroundings.

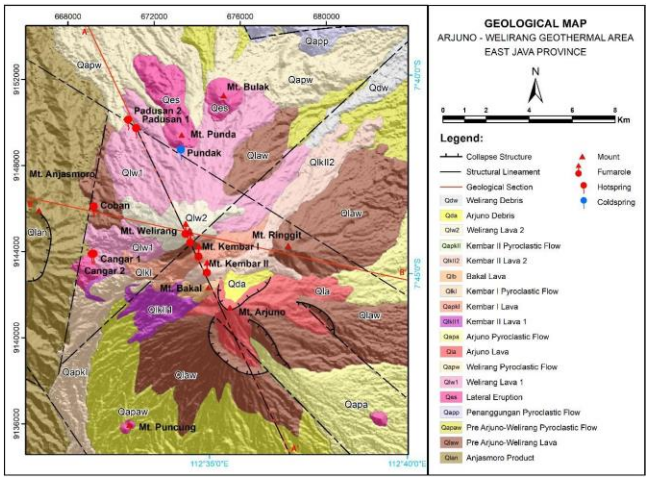

Figure 1. Geological Map of the Arjuno-Welirang Volcanic Area[16]

These areas are composed of rock units resulting from volcanic activity from several different eruption centers, which are classified by their geological age. The oldest formation originated from Mount Anjasmoro and formed during the early Pleistocene. Next, volcanic deposits from the Ringgit-Pundak-Butak volcanoes formed during the Middle Pleistocene. Finally, volcanic activity at the end of the Pleistocene formed the Arjuno-Welirang-Kembar I and II volcano complexes. The youngest eruption products originate from Mount Penanggungan, formed during the Holocene [17].

The Arjuno-Welirang Area region has a complex geological structure characterized by normal faults, strike-slip faults, caldera rim structures, and subsidence zones. The fault patterns in this area generally cut directly through the mountain body, primarily oriented north-south, northwest-southeast, southwest-northeast, and west-east. The caldera rim structure is located in the central part of the volcanic complex, indicating significant ancient volcanic activity. A subsidence zone has been identified in the southern sector of the Arjuno-Welirang peak. It opens toward the southeast and northeast, indicating deformation caused by the interaction of volcanic and tectonic processes [18]. The presence of geothermal energy sources beneath the surface of the area is indicated by the emergence of hot springs in the western part of the Arjuno-Welirang area, such as in Cangar, Padusan, and Coban. While the volcanic rocks in this region are generally Quaternary in age, further exploration of the potential for heat sources in the form of hot igneous rocks and magmatic intrusions could support the development of geothermal energy [19].

Materials and Methods

The gravity method used in this study is based on Newton's Law of Universal Gravitation, which states that gravitational force is proportional to the product of two masses and inversely proportional to the square of the distance between them [20]. Mathematically, we can formulate this principle as follows:

$$\vec{F}_{12} = -G\frac{m_1 m_2}{r^2}\vec{r}_{12} \quad (1)$$

In geophysical applications, variations in the measured gravitational field are primarily controlled by lateral and vertical contrasts in subsurface mass density [21]. Therefore, gravity data are widely used to infer subsurface geological structures. However, gravity measurements generally contain contributions from multiple sources, including non geological effects, which must be corrected and processed to isolate anomalies related to subsurface density variations [22].

The study area is located in the Arjuno-Welirang Mountain region, with geographical coordinates 112°31′22″E – 112°39′1.2″E and 7°48′49″N – 7°39′1.7″N. This study uses GGMPlus gravity model data, which can be downloaded from the website https://ddfe.curtin.edu.au/gravitymodels/GGMplus/, GGMplus provides high resolution gravity field data with an approximate spatial resolution of 200 m, enabling detailed detection of subsurface density contrasts relevant to geothermal exploration [23]. The gravity data obtained from the GGMPlus model is free air anomaly data [24]. Since FAA only considers the elevation difference between the measuring instrument and the datum level, additional corrections are needed to obtain the Complete Bouguer Anomaly (CBA) value. The CBA value also accounts for the mass above or below the datum surface that is influenced by topographic variations and surface mass distribution [25]. Therefore, a Bouguer correction process is required to obtain the Complete Bouguer Anomaly (CBA), calculated using Microsoft Excel 2019 software based on the following equation:

$$BC = 0.04193\rho h \quad (2)$$

Bouguer Correction (BC) is expressed in milligals (mGal) and is calculated based on the rock density (ρ) and the elevation of the study area (h). The rock density, denoted by ρ, is measured in grams per cubic centimeter (g/cm³) and represents the density of the subsurface material in the region. Elevation (h), measured in meters (m), is a critical factor in the correction process as it contributes to the gravitational effect that must be accounted for. The optimum Bouguer density was determined using the Parasnis method, which is based on the linear relationship between free air anomaly and Bouguer slab correction. In this method, the density value is obtained by minimizing the correlation between FAA and elevation, thereby reducing the influence of topographic effects and yielding a representative average density for gravity data reduction [26]. This estimate is then used in terrain correction to overcome the effects of uneven mass distribution around the measurement location. Terrain correction accounts for the gravitational effect of surrounding topography, including hills and valleys, which may either increase or decrease the observed gravity value depending on their relative position to the measurement point [27]. Therefore, the measured gravity value must be corrected for terrain. Terrain correction is performed using Oasis Montaj and Global Mapper software. The Complete Bouguer Anomaly (CBA) value can be calculated using the following equation once the Bouguer correction and terrain correction values are obtained [25] is calculated using the equation:

$$CBA = FAA - BC + TC \quad (3)$$

The gravitational force values at a given point on Earth can differ from the surrounding values due to variations in mass density beneath the surface. Gravity field anomalies are defined as the difference

between the measured and theoretical gravity field values at a given point on the surface [28]. The Complete Bouguer Anomaly (CBA) is expressed in milligals (mGal) and is obtained by considering several gravity correction components the free air anomaly (FAA), Bouguer correction (BC), and terrain correction (TC). CBA contour maps are used to identify anomalies near and far from the surface, including residual, regional, and noise anomalies that cause interaction and overlap [29]. Therefore, an anomaly separation method using Butterworth filtering is required. After filtering with the Butterworth filter, regional and residual anomaly contour maps are obtained [30]. Anomaly separation was conducted using a Butterworth filter with a cutoff wavelength of 7.25 km and a filter order of 23. The resulting regional anomaly reflects gravity responses from deeper sources, whereas the residual anomaly was calculated as the difference between the Complete Bouguer Anomaly (CBA) and the regional anomaly, representing shallow density variations [31].

The first horizontal derivative (FHD), also known as the horizontal gradient (HG), is a method used to determine the location of horizontal density contrast boundaries based on gravity data. It is the first derivative of the gravity anomaly value in the horizontal direction [32]. The FHD method detects lateral changes in the gravity field caused by variations in density contrast at the boundaries of geological structures. Gravity anomalies produced by an object tend to show significant changes in gradient at its edges [33] following the equation:

$$FHD = \sqrt{\left(\frac{\partial g}{\partial x}\right)^2 + \left(\frac{\partial g}{\partial y}\right)^2} \quad (4)$$

The FHD value will reach its maximum when there are striking differences in gravity anomalies at object boundaries or between layers. This maximum value can be used to indicate the presence of geological boundaries based on measured gravity data [34]. The next step was to use the Second Vertical Derivative (SVD) method to analyze the data. Applying the SVD method to Bouguer anomaly data aims to separate the effects of shallow and deep structures [35]. The SVD method clarifies zero anomaly information contained in gravity data. A value of 0 mGal/m² indicates lateral density contrast, often associated with faults [36]. The SVD value is determined by calculating the second derivative using the following equation [37]:

$$SVD = \frac{g_{(i-1)} - 2g_{(i)} + g_{(i-1)}}{(\Delta x)^2} \quad (5)$$

The Second Vertical Derivative (SVD) was applied to highlight lateral density contrasts, and faults or fractures were identified from sign changes and zero-crossing patterns of the SVD anomalies on the residual gravity map [38]. Subsequently, profile slicing was performed along zones with significant anomaly contrasts to support further structural interpretation. Fault zones were interpreted from the distribution and polarity of positive and negative SVD anomalies, which indicate sharp density contrasts related to faulted structures [39].

The next step is Inversion modelling, Inversion modelling is often referred to as the opposite of forward modeling, as in inversion modeling, the subsurface model is derived directly from observational data. Inversion theory encompasses a set of mathematical and statistical techniques aimed at extracting useful information about a physical system based on observations of that system. The physical system refers to the phenomenon under investigation, the observation refers to the collected data, and the information to be derived from the data constitutes the model or its associated parameters [40].

In the inversion process, field data are typically analyzed by performing curve fitting between the observed data and the mathematical model. The primary objective of the inversion method is to estimate the physical parameters of subsurface conditions that are not directly observable. Inversion modeling techniques for gravity anomaly data have been widely applied, both to corrected primary gravity anomaly data and to regional and residual anomaly data, as well as to complete Bouguer anomaly datasets [41]. Therefore, in this study, inversion methods were employed for subsurface modeling purposes.

The inversion results for the study area were obtained by modeling the local gravity anomaly data down to a depth of approximately ±3000 meters. Data processing was conducted using the ZondGM2D software, which involved generating two cross-sectional profiles oriented west-east (W-E) and northwest-southeast (NW-SE). Based on the modeling results, subsurface density boundaries were interpreted along with the identification of potential heat source zones associated with the geothermal system in the area.

Results and Discussion

Complete Bouguer Anomaly of the Arjuno-Welirang Volcanic Area

The Complete Bouguer Anomaly map shown in Figure 2(a) indicates that gravity anomaly values in the study area range from −23 to 61.9 mGal. For interpretation purposes, the gravity anomalies were classified into three categories (low, moderate, and high) based on the distribution of anomaly values and their geological relevance. Low gravity anomalies, ranging from −23 to less than 18.8 mGal, are predominantly distributed in the central to southern parts of the study area and indicate low density zones that are likely composed of altered rocks, sediments, fractures, and steam pockets associated with geothermal systems. Moderate gravity anomalies, ranging from 18.8 to less than 40.5 mGal, are observed in the southwestern and northeastern regions and are interpreted as fractured volcanic rocks that may serve as pathways for the migration of geothermal fluids. High gravity anomalies, with values greater than or equal to 40.5 mGal up to 61.9 mGal, are mainly located in the northwestern part of the area and are associated with high-density rocks, such as igneous intrusions. These intrusions are interpreted as potential heat sources within the Arjuno-Welirang geothermal system.

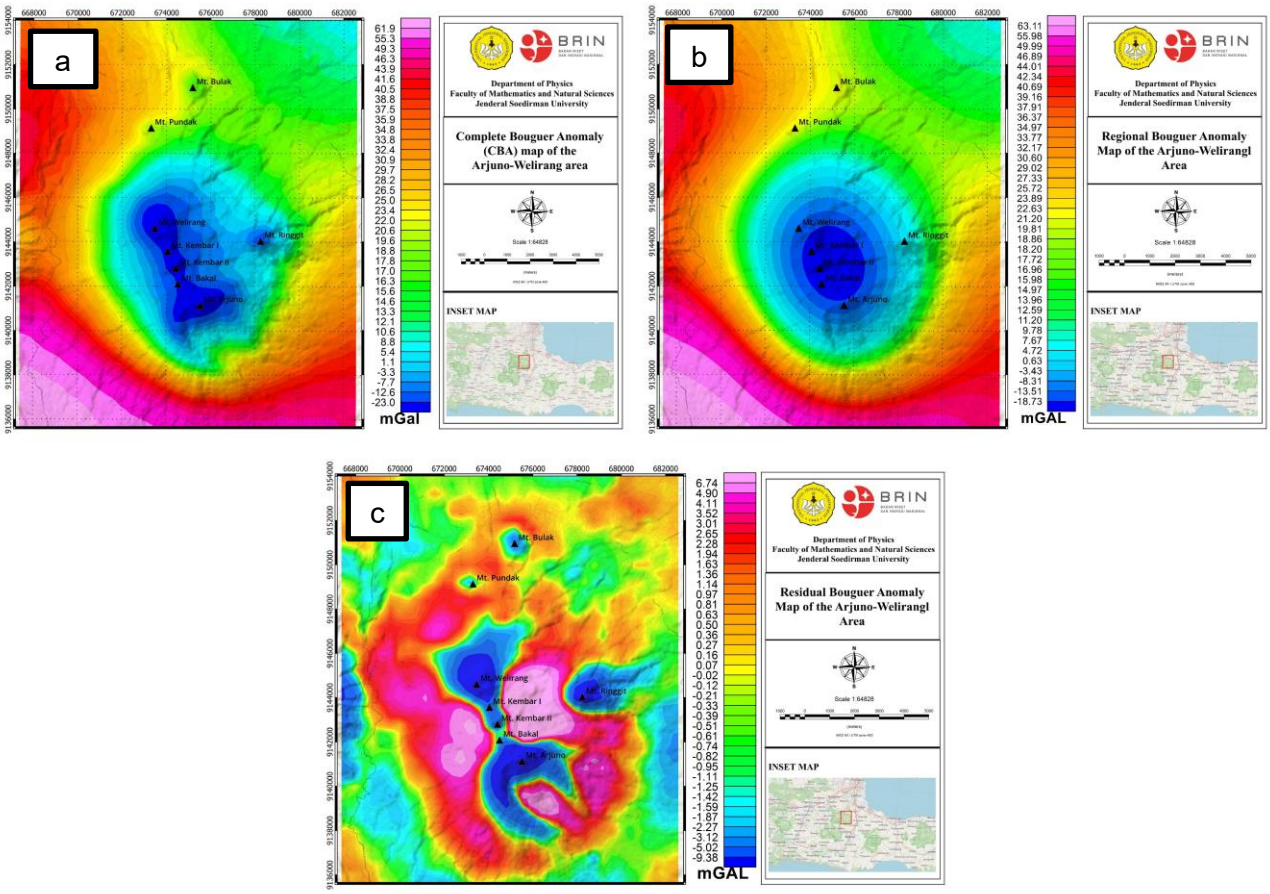

Figure 2. Gravity anomaly maps of the Arjuno-Welirang volcanic complex:(a) Complete Bouguer Anomaly, (b) Regional Anomaly, (c) Residual Anomaly

Regional and Residual Anomalies of the Arjuno-Welirang Area

Separating the regional components from the complete Bouguer anomaly provides more information about the density distribution at intermediate depths. The results show that the gravity anomaly values in the study area range from -18.73 to 63.11 mGal. The low anomaly zone (-18.73 to 7.67 mGal) distributed across the central and southeastern regions, indicates the presence of low-density materials, such as altered rock or fracture zones. The moderate anomaly zone (7.67 to 29.02 mGal) is located in the northwest and southwest and reflects a transition zone likely traversed by pathways of hot fluid migration. The high anomaly zone (29.02 to 63.11 mGal) is found in the west and northeast and is associated with intrusive igneous rocks that serve as the heat source of the geothermal system.

Residual anomaly analysis, which represents shallow geological conditions, shows values ranging from -9.38 to 6.74 mGal. The low anomaly zone (-9.38 to -1.42 mGal) is distributed around Mount Arjuno and Mount Welirang, which associated with altered volcanic rocks and fracture zones that serve as migration pathways for geothermal fluids. The moderate anomaly zone (1.14 to 6.74 mGal) lies between the low and high zones and reflects lithological transitions, being influenced by structures such as the Padusan and Ledug faults. The high anomaly zone (1.14 to 6.74 mGal) is in the western and northeastern regions and is believed to be the location of high-density igneous rock intrusions that are the heat source of the Arjuno–Welirang geothermal system.

Derivative Analysis of the Arjuno-Welirang Volcanic Area

The presence of fault structures in the study area was analyzed using the First Horizontal Derivative (FHD) method shown in Figure 3 (a) and the Second Vertical Derivative (SVD) method shown in Figure 3 (b). The correlation graph in the "Second Vertical Derivative" and "First Horizontal Derivative Anomaly" sections can be used to identify areas identified as fault zones. In analyzing the presence of subsurface geological structures, important aspects to consider are the zero contour values in the SVD anomaly and the maximum values in the FHD [42]. The SVD technique was employed due to its capability to clearly highlight density contrast boundaries, thereby enabling effective identification of fault structures in the study area. In Figure 3 (b), the SVD contour map shows the contrast between areas with high and low anomalies. These anomalies can be interpreted as an indication of the presence of fault structures beneath the surface.

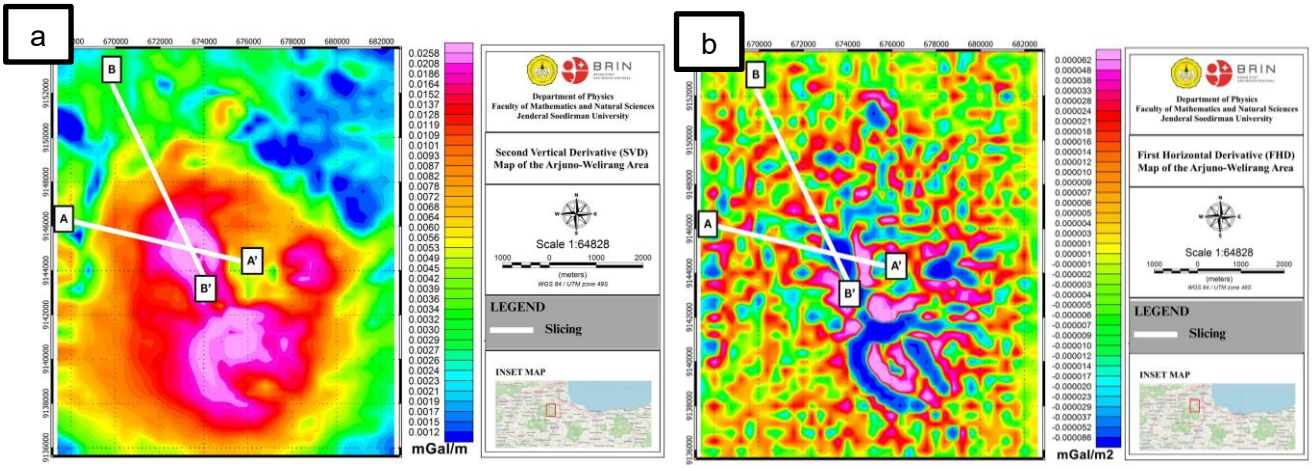

Figure 3. Derivative Analysis: (a) First Horizontal Derivative (FHD) Map, (b) Second Vertical Derivative (SVD) Map

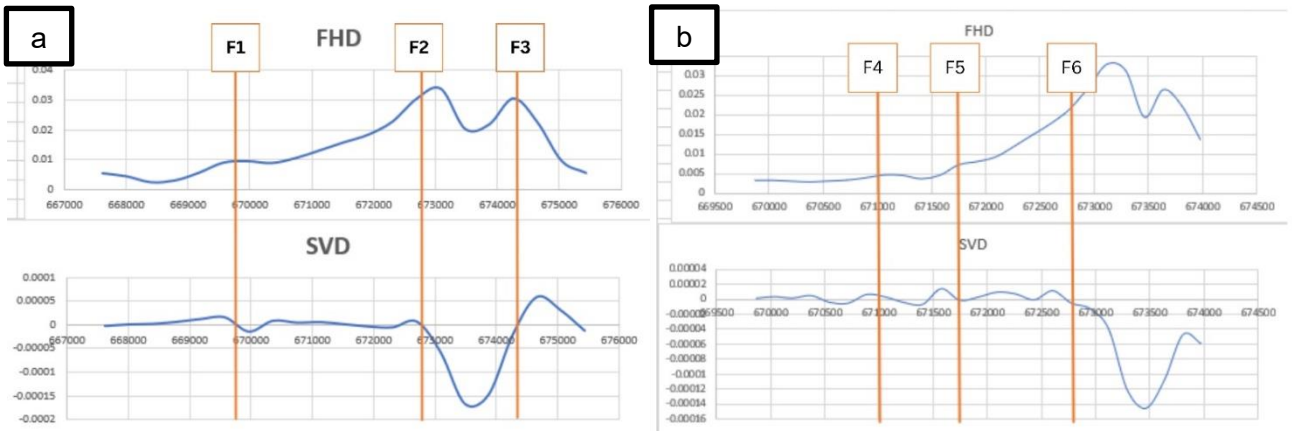

Figure 4. a) FHD and SVD profiles along cross-section A–A′, b) FHD and SVD profiles along cross-section B–B′

In gravity derivative analysis, structural boundaries such as faults and lithological contacts can be effectively highlighted using the FHD and SVD of the gravity field. Maximum values in the FHD map are commonly interpreted as zones of sharp lateral density contrast, which are typically associated with fault contacts or structural discontinuities. Meanwhile, zero crossing zones in the SVD map represent transitions between positive and negative curvature of the gravity anomaly and are widely interpreted as the surface projection of fault planes or major subsurface structural boundaries. As illustrated in Figure 4, the alignment between FHD maxima and SVD zero crossing zones provides a robust basis for delineating fault structures within the study area [43].

The interpretation of the residual gravity anomaly map overlaid with fault structures derived from SVD analysis and geological data reveals a strong correlation between fault zones and the presence of geothermal manifestations in the Arjuno-Welirang area. Several identified faults, such as F1 and F4, are located near geothermal manifestations in the form of hot springs at Coban and Padusan, respectively. Meanwhile, faults F2, F3, and F6 are situated around the summit of Mount Welirang, where significant fumarolic and solfataric activities occur. These fault structures are inferred to act as migration pathways for hydrothermal fluids, indicating that the geothermal system's outflow zone is situated in the southwestern part of the study area [44]. This interpretation is consistent with the conceptual models proposed by Daud *et al*. [34] and Hadi *et al*. [35], which suggest that the upflow zone is located beneath the Mount Welirang volcanic complex, as evidenced by a dome-shaped resistivity structure and the presence of surface fumarolic activity.

The outflow zones are distributed toward the west and northwest, in alignment with the occurrence of bicarbonate hot springs at Coban, Cangar, and Padusan, as depicted in Figure 5. These are structurally controlled by major faults, such as the Ledug Fault (west-east direction) and the Padusan Fault (northwest–southeast direction). Overall, the structural interpretation based on gravity data in this study supports the existing conceptual models and reinforces the critical role of geological structures in controlling subsurface fluid dynamics within the Arjuno–Welirang geothermal system.

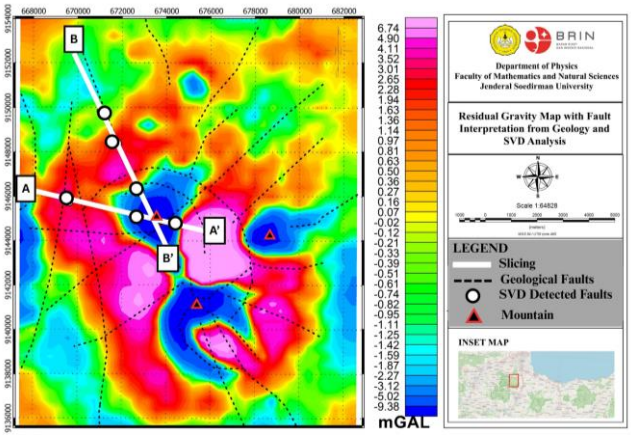

Figure 5. Residual Bouguer gravity anomaly map of the Arjuno–Welirang geothermal area with fault interpretations derived from derivative analysis and geological data

2D Subsurface Structural Modeling of the Arjuno-Welirang Volcanic Area

The results of the 2D gravity modeling along the A–A′ cross-section, which extends west to east from the Coban Hot Springs to Mount Welirang, reveal subsurface structures that are closely associated with the Arjuno–Welirang geothermal system. The model delineates three primary zones based on variations in rock density.

The first zone is characterized by low-density values (approximately 2.00–2.30 g/cm³) and dominates the subsurface region beneath Mount Welirang, extending westward toward the Coban Hot Springs. This zone is interpreted as a clay alteration cap formed by sustained hydrothermal activity. Such layers are typically conductive and impermeable, acting as a seal above geothermal reservoirs. Notably, this zone exhibits a dome-shaped geometry beneath Mount Welirang, a common morphological indicator of an upflow zone in geothermal systems [44]. The second zone represents an intermediate-density region (approximately 2.30–2.55 g/cm³) situated beneath the clay cap. This zone is interpreted as the geothermal reservoir, consisting of relatively compact rock with sufficient porosity and fracturing to permit the storage and migration of thermal fluids. This interpretation is further supported by magnetotelluric (MT) inversion results, which reveal resistivity values ranging from 20 to 60 ohm·m at corresponding depths and locations typical of geothermal reservoir rocks. Lithologically, this zone aligns with the old Arjuno–Welirang lava unit (Qltaw) and Welirang lava unit (Qlw), which consist of porphyritic andesitic to basaltic lava. These rock types are relatively permeable and capable of retaining geothermal fluids.

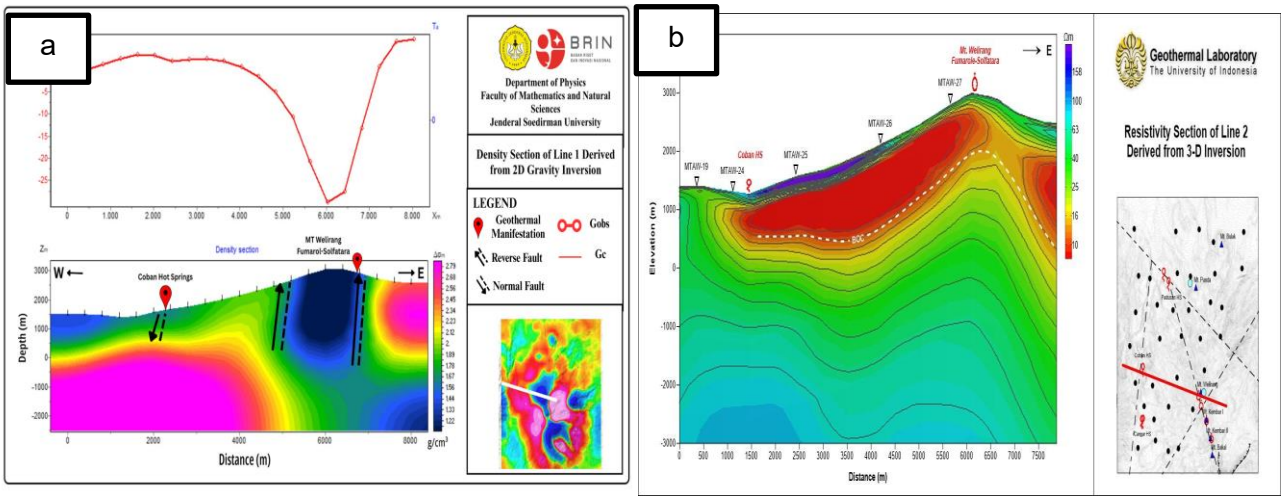

Figure 6. a) 2D gravity inversion modeling section along Line 1, b) Resistivity section derived from 3D magnetotelluric (MT) inversion[45]

The high density zone (>2.60 g/cm³) identified beneath Mount Welirang at depths greater than 1.5 km is interpreted as a magmatic intrusive body that serves as the primary heat source of the Arjuno–Welirang geothermal system. This interpretation is consistent with previous studies based on Magnetotelluric (MT) data, which indicate high resistivity values at similar depths and locations, characteristic of intrusive and unaltered rocks[45].

In addition, the relatively low-density zone observed near the surface around the Coban Hot Springs is interpreted as an outflow zone [16], where geothermal fluids migrate laterally from the upflow region before discharging at the surface. This interpretation is also in agreement with MT based interpretations reported in reference [45], which associate conductive layers in this area with geothermal outflow processes. Collectively, the results of this gravity-based interpretation demonstrate a high degree of coherence with established regional geological models and prior geophysical investigations, particularly MT studies. No significant discrepancies were identified, and the gravity inversion model offers enhanced resolution of both vertical and lateral subsurface structures, which are often not discernible from surface geological data alone. Consequently, it may be concluded that the 2D gravity inversion effectively characterizes the Arjuno–Welirang geothermal system and significantly contributes to a more comprehensive understanding of the spatial configuration and interrelation among the upflow, reservoir, and outflow zones.

The B–B′ profile represents a northwest-southeast oriented cross section across the Arjuno–Welirang geothermal area, designed to intersect major structural trends and surface geothermal manifestations. This trajectory is expected to capture key subsurface features related to fluid pathways, alteration zones, and heat sources within the geothermal system. The results of the 2D gravity inversion along the B–B′ profile are presented in Figure 7.

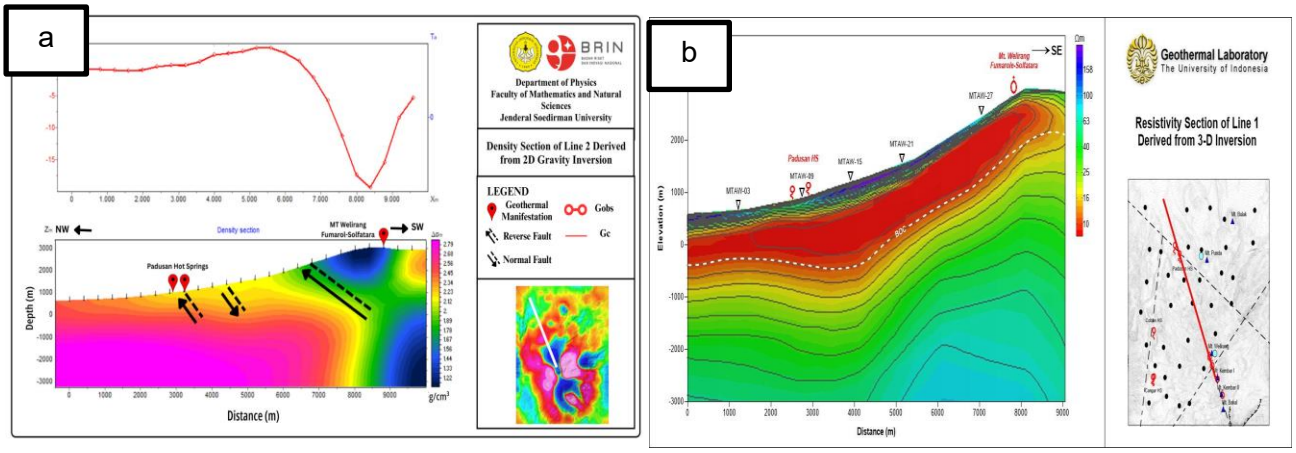

Figure 7. a) 2D gravity inversion modeling section along Line 2, b) Resistivity section derived from 3D magnetotelluric (MT) inversion[45]

The interpretation of the 2D gravity inversion modeling along the B–B′ profile (northwest to southeast), as illustrated in Figure 7 (a), within the Arjuno–Welirang geothermal area, predominantly reveals subsurface structures that support the existence of an active geothermal system. The primary focus of this analysis is to delineate low-density zones, indicative of hydrothermal alteration and potential geothermal reservoirs, as well as high-density zones associated with intrusive igneous bodies that function as the system's heat source. Validation of this model is performed through comparison with previous Magnetotelluric (MT) studies.

Based on the gravity inversion results, three main density zones are identified: (1) a low-density zone (<2.3 g/cm³) extending from the Padusan Hot Springs area to the western flanks of Mt. Welirang, (2) an intermediate-density zone (2.3–2.5 g/cm³) at mid crustal depths, and (3) a high-density zone (>2.6 g/cm³) prominently located at greater depths beneath Mt. Welirang. The low-density zone is associated with hydrothermal alteration and is interpreted as a clay cap layer. This interpretation is strongly supported by MT data, which identify a conductive layer with resistivity values ranging from 1 to 10 ohm·m that thickens towards Padusan and Coban [45]. The clay cap is believed to have formed through intensive hydrothermal alteration processes in the upper part of the system and serves as a sealing layer that confines geothermal fluids beneath it.

Further southeast, directly beneath Mt. Welirang, the gravity model reveals a very low-density structure with an up-dome geometry extending toward shallow depths. This feature is interpreted as the upflow pathway for geothermal fluids, consistent with the MT model, which shows a high-resistivity anomaly, suggesting the presence of a hot magmatic intrusion At the surface, this dome structure coincides with active geothermal manifestations, including intense fumarolic and solfataric activity at the summit of Mt. Welirang. This zone is therefore interpreted as the core of the geothermal system, where deep-seated fluids ascend toward the surface.

The presence of several fault structures along the gravity profile, particularly in the Padusan area and the flanks of Mt. Welirang, further supports the role of geological structures as migration pathways for hydrothermal fluids. These faults facilitate the ascent of fluids from the reservoir zone to the surface, giving rise to manifestations such as the Padusan Hot Springs. The intermediate density zone, located between the low and high density regions, most likely represents the geothermal reservoir rocks. This interpretation is corroborated by the MT model, which indicates resistivity values ranging from 20 to 60 ohm·m, situated directly beneath the clay cap and above the heat source zone [45].

The gravity model successfully delineates the subsurface architecture of the Arjuno–Welirang geothermal system, revealing the geological structure pattern comprising an upflow zone beneath Mt. Welirang, an outflow pathway extending toward Padusan, and clear indications of a clay cap and

geothermal reservoir consistent with a high-temperature system. However, it should be acknowledged that gravity inversion alone cannot uniquely resolve subsurface structures due to its inherent non-uniqueness, whereby different density distributions may produce similar gravity responses[46]. Although joint inversion was not performed in this study, the gravity-derived density model was systematically compared with magnetotelluric (MT) models reported in previous investigations. The strong correspondence between density variations and resistivity structures provides independent validation of the gravity interpretation and helps constrain the identification of key geothermal system components, including the cap rock, reservoir, and heat source.

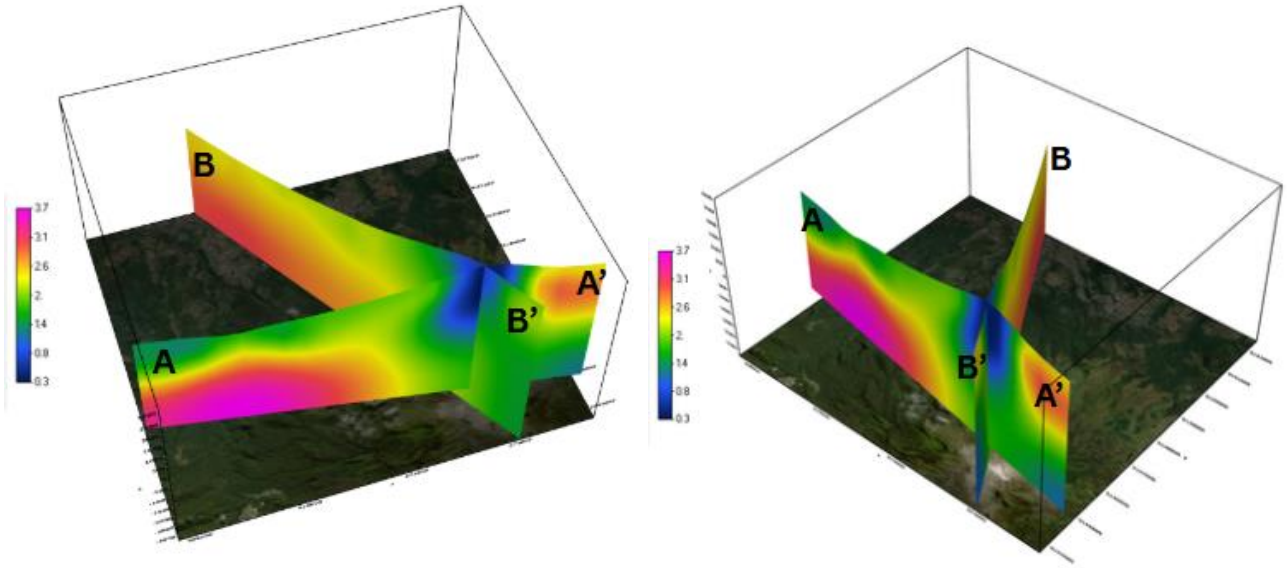

Figure 8. 3D fence diagram constructed from gravity inversion sections along Lines A–A′ and B–B′

Following the gravity inversion modeling along profiles A–A′ and B–B′, a 3D fence diagram was constructed by integrating both cross-sections to obtain a more comprehensive spatial visualization of the subsurface geometry. As shown in Figure 8, the fence diagram was developed by intersecting profile A with the orthogonally oriented profile B. The primary objective of this construction is to delineate the geometric relationships among density anomaly zones within the Arjuno–Welirang geothermal system.

The integrated model reveals a dome-shaped low-density structure (<2.3 g/cm³), interpreted as the upflow zone, consistently located at the intersection of profiles A and B directly beneath Mount Welirang. This orthogonal configuration reinforces the interpretation of a well organized 3 dimensional geothermal architecture, exhibiting both vertical and lateral connectivity among key subsurface zones. The resulting fence diagram plays a crucial role in enhancing the conceptual understanding of the geothermal system and supports multi-profile integration for detailed subsurface mapping.

Conclusions

In conclusion, the results indicate the presence of a well developed geothermal system beneath the Arjuno–Welirang volcanic area. The analysis of the First Horizontal Derivative (FHD) and Second Vertical Derivative (SVD) of gravity data successfully identified six major fault structures in the Arjuno–Welirang geothermal area, comprising four normal faults and two reverse faults. These faults play a crucial role as conduits for hydrothermal fluid migration, particularly around Padusan and the flanks of Mount Welirang, where surface geothermal manifestations such as hot springs and fumaroles are observed. The 2D gravity inversion modeling along profiles A–A′ and B–B′ delineates three primary subsurface density zones: a low-density zone (<2.3 g/cm³) interpreted as a clay cap formed by hydrothermal alteration; an intermediate-density zone (2.3–2.5 g/cm³) representing permeable reservoir rocks; and a high-density zone (>2.6 g/cm³) associated with magmatic intrusions acting as the heat source. A dome shaped structure beneath Mount Welirang indicates an upflow zone, while the area toward Padusan is interpreted as an outflow pathway. These interpretations are consistent with previous magnetotelluric (MT) studies, reinforcing the characterization of Arjuno–Welirang as a high temperature geothermal system. These findings provide important constraints for future geothermal exploration, indicating that zones characterized by low-density reservoirs intersected by major fault systems represent promising targets for drilling and geothermal development.

Conflicts of Interest

The authors declares that there is no conflict of interest regarding the publication of this paper.

Acknowledgment

The authors thank BRIN's Research Center for Limnology and Water Resources for satellite data support, Universitas Jenderal Soedirman for institutional and academic contributions essential to the success of this study, and PT Pro Tech Engineering for research funding support.

References

[1] Ermawati, T., Dwiastuti, I., Purwanto, & Negara, S. D. (2014). *Analisis kebijakan pengembangan energi panas bumi di Indonesia*.
[2] Saraswati, G. P., Prasetyo, Y., & Sukmono, A. (2019). Analisis estimasi energi panas bumi dan rekomendasi lokasi pembangkit listrik tenaga panas bumi menggunakan citra Landsat 8 (studi kasus: Kawasan Gunung Ungaran, Jawa Tengah). *Jurnal Geodesi Undip, 8*(1), 170–179.
[3] Mokom, N., Ujah, C., Christian, A., & Kallon, D. (2025). Exploring geothermal energy as a sustainable source of energy: A systemic review. *Unconventional Resources, 6*, 100149. https://doi.org/10.1016/j.uncres.2025.100149.
[4] Domra Kana, J., Djongyang, N., Raïdandi, D., Njandjock Nouck, P., & Dadjé, A. (2015). A review of geophysical methods for geothermal exploration. *Renewable and Sustainable Energy Reviews, 44*, 87–95. https://doi.org/10.1016/j.rser.2014.12.026.
[5] Meilasandi, T., Sugianto, A., Indriana, R. D., & Harmoko, U. (2019). 3D gravity data modelling for determining a subsurface structure of the SDP geothermal field. *Journal of Physics: Conference Series, 1217*(1), 012042. https://doi.org/10.1088/1742-6596/1217/1/012042.
[6] Pocasangre, C., Fujimitsu, Y., & Nishijima, J. (2020). Interpretation of gravity data to delineate the geothermal reservoir extent and assess the geothermal resource from low-temperature fluids in the municipality of Isa, southern Kyushu, Japan. *Geothermics, 83*, 101735. https://doi.org/10.1016/j.geothermics.2019.101735.
[7] Karimah, N. A., Supriyadi, S., & Suprianto, A. (2021). Korelasi data gravitasi satelit pada daerah panas bumi Blawan–Ijen. *Jurnal Sains Dasar, 9*(1), 11–15. https://doi.org/10.21831/jsd.v9i1.26431.
[8] Martha, A. A., Setiawan, A., & Setiadi, T. A. P. (2023). Utilization of global gravity model plus (GGMPlus) to identify fault structures in Mamasa District, West Sulawesi. *AIP Conference Proceedings, 2941*(1), 030006. https://doi.org/10.1063/5.0181519.
[9] Fauzik, D., Haris, A., Martha, A. A., & Riyanto, A. (2020). Liquefaction potential identification in Central Sulawesi using gravity inversion model. *IOP Conference Series: Earth and Environmental Science, 538*(1), 012035. https://doi.org/10.1088/1755-1315/538/1/012035.
[10] Juwita, W., Juventa, J., Setiawan, A. M., Martha, A. A., Hudayat, N., & Sutedja, B. (2024). Identification of potential hydrocarbon traps using the gravity method in the Bengkulu Basin. *Iranian Journal of Geophysics, 18*(3), 69–83. https://doi.org/10.30499/ijg.2023.409882.1535.
[11] Rahman, S. A. N., Martha, A. A., Sutrisno, S., Wulandari, A., & Hudayat, N. (2025). Identification of subsurface structures and potential reservoir zones of geothermal fields based on gravity data analysis in the Karaha–Cakrana area, West Java. *Iranian Journal of Geophysics, 19*(3), 63–76. https://doi.org/10.30499/ijg.2024.434652.1563.
[12] Wahyuningsih, R. (2005). *Kolokium hasil lapangan–DIM* (pp. 1–9).
[13] Wahyuningsih, R. (n.d.). *Potensi dan wilayah kerja pertambangan panas bumi di Indonesia*.
[14] Lita, F. (2012). *Identifikasi anomali magnetik di daerah prospek panas bumi Arjuna–Welirang* (Undergraduate thesis). Universitas Indonesia.
[15] Suharno, Nindya, F., Rustadi, Zaenuddin, A., & Mulyatno, B. S. (2013). Characteristics of Mountain Arjuno–Welirang geothermal, East Java Province, Indonesia. *Proceedings of the 13th Indonesian International Geothermal Convention & Exhibition*.
[16] Daud, Y., Fahmi, F., Nuqramadha, W. A., Heditama, D. M., Pratama, S. A., & Suhanto, E. (2015). 3-dimensional inversion of MT data over the Arjuno–Welirang volcanic geothermal system, East Java (Indonesia). *Proceedings of the World Geothermal Congress 2015*.
[17] API, P. B. D. I. K. G., & Welirang, A. (2016). *Studi vulkanisme dan struktur geologi untuk eksplorasi awal*.
[18] Nidya, F., Suharno, Zarkasyi, A., & Sugianto, A. (2013). Analisis karakteristik panas bumi daerah outflow Gunung Arjuno–Welirang berdasarkan data geologi, geokimia, dan geofisika (3G). *Jurnal Geofisika Eksplorasi, 1*(2), 7.
[19] Sumotarto, U. (2018). Geothermal energy potential of Arjuno and Welirang volcanoes area, East Java, Indonesia. *International Journal of Renewable Energy Research, 8*(1), 614–624. https://doi.org/10.20508/ijrer.v8i1.6690.g7336.
[20] Indriana, R. D., Kirbani, S. B., Setiawan, A., & Sunantyo, T. A. (2018). Gravity observation data analysis 1988–1998–2011 to determine gravity changes of Merapi Volcano. *Journal of Physics: Conference Series, 983*(1), 012042. https://doi.org/10.1088/1742-6596/983/1/012042.
[21] Araffa, S. A. S., *et al*. (2018). Implementation of magnetic and gravity methods to delineate the

subsurface structural features of the basement complex in central Sinai area, Egypt. *NRIAG Journal of Astronomy and Geophysics, 7*(1), 162–174. https://doi.org/10.1016/j.nrjag.2017.12.002.
[22] Anggraeni, F. K. A., & Sulistyorini. (2021). Two-dimensional modeling (2D) gravity method for interpreting subsurface structure of Mount Merapi. *Journal of Physics: Conference Series, 1832*(1), 012002. https://doi.org/10.1088/1742-6596/1832/1/012002.
[23] Permana, N. R., & Gunawan, B. (2024). Estimations of the geothermal energy potential in the Mount Anak Krakatau region based on derivative analysis and 3D model of gravitational satellite data, *7*(1), 43–57.
[24] Hirt, C., Claessens, S., Fecher, T., Kuhn, M., Pail, R., & Rexer, M. (2013). New ultrahigh-resolution picture of Earth's gravity field. *Geophysical Research Letters, 40*(16), 4279–4283. https://doi.org/10.1002/grl.50838.
[25] Awaliyah, A., & Pohan, A. F. (2024). Perbandingan koreksi medan (terrain correction) konvensional dan modern pada metode gravitasi menggunakan data DEM ERTM2160 dan SRTM2gravity pada wilayah Cianjur. *Jurnal Fisika Unand, 13*(5), 651–657. https://doi.org/10.25077/jfu.13.5.651-657.2024.
[26] Parasnis, D., & Cook, A. H. (1952). A study of rock density in the English Midlands. *Geophysical Journal International, 6*, 252–271. https://doi.org/10.1111/j.1365-246X.1952.tb03013.x.
[27] Hinze, W., *et al*. (2005). New standards for reducing gravity data: The North American gravity database. *Geophysics, 70*(4). https://doi.org/10.1190/1.1988183.
[28] Sarkowi, M. (2014). *Eksplorasi gaya berat*. Graha Ilmu.
[29] Purnomo, J., Koesuma, S., & Yunianto, M. (2016). Pemisahan anomali regional–residual pada metode gravitasi menggunakan metode moving average, polynomial, dan inversion. *Indonesian Journal of Applied Physics, 3*(01), 10. https://doi.org/10.13057/ijap.v3i01.1208.
[30] Anggraeni, F. K. A. (2023). Identifikasi struktur bawah permukaan Gunung Semeru pasca erupsi tahun 2022. *Jurnal Ilmu dan Inovasi Fisika, 7*(1), 69–77. https://doi.org/10.24198/jiif.v7i1.40885.
[31] Mickus, K., Aiken, C., & Kennedy, W. (1991). Regional–residual gravity anomaly separation using the minimum-curvature technique. *Geophysics, 56*, 279–283. https://doi.org/10.1190/1.1443041.
[32] Juwita, W., Juventa, J., Setiawan, A. M., Martha, A. A., Hudayat, N., & Sutejo, B. (2024). Identification of potential hydrocarbon traps using the gravity method in the Bengkulu Basin. *Iranian Journal of Geophysics, 18*(3), 69–83. https://doi.org/10.30499/ijg.2023.409882.1535.
[33] Wijanarko, E., Sunarjanto, D., & Dian Nur, D. N. (2021). Identifikasi struktur geologi bawah permukaan menggunakan metode horizontal gradient, Euler deconvolution, dan second vertical derivative: Studi eksplorasi panas bumi Baturaden, Jawa Tengah. *Lembaran Publikasi Minyak dan Gas Bumi, 55*(1), 25–35. https://doi.org/10.29017/lpmgb.55.1.574.
[34] Fitriastuti, A., Aristo, & Putri, F. F. (2019). Identifikasi struktur bawah permukaan menggunakan metode gaya berat analisis first horizontal derivative (FHD) dan second vertical derivative (SVD) guna mitigasi bencana gempabumi di Kabupaten Wonosobo. *Prosiding Seminar Nasional Kebumian ke-12*, 604–614.
[35] *Pemodelan tiga dimensi anomali gravitasi dan identifikasi sesar lokal dalam penentuan jenis sesar di daerah Pacitan* (n.d.).
[36] Ibrahim, M. M., Utami, P., & Raharjo, I. B. (2022). Analisis struktur geologi berdasarkan data gravitasi menggunakan metode second vertical derivative (SVD) pada lapangan panas bumi "X." *Jurnal Geosains dan Remote Sensing, 3*(2), 59. https://doi.org/10.23960/jgrs.2022.v3i2.76.
[37] Zaenudin, A., & Yulistina, S. (2020). Studi identifikasi struktur geologi bawah permukaan untuk mengetahui sistem sesar berdasarkan analisis FHD, SVD, dan pemodelan forward 2.5D di daerah Manokwari, Papua Barat. *Jurnal Geofisika Eksplorasi, 4*(2), 173–186. https://doi.org/10.23960/jge.v4i2.15.
[38] Blakely, R. J., & Simpson, R. W. (1986). Approximating edges of source bodies from magnetic or gravity anomalies. *Geophysics, 51*(7), 1494–1498. https://doi.org/10.1190/1.1442197.
[39] Telford, W. M., Geldart, L. P., & Sheriff, R. E. (1990). *Applied geophysics* (2nd ed.). Cambridge University Press.
[40] Grandis, H. (2009). *Pengantar pemodelan inversi geofisika*. Himpunan Ahli Geofisika Indonesia.
[41] Permana, N. R., Gunawan, B., & Nafian, M. (2022). Analysis of subsurface structure of Sembalun geothermal prospect area, East Lombok, with 2D and 3D gravity modeling. *Al-Fiziya Journal of Materials Science, Geophysics, Instrumentation and Theoretical Physics, 5*(1), 10–22. https://doi.org/10.15408/fiziya.v5i2.24943
[42] Safira, A., Saipuddin, M., Andita, Z. A., & Catur, R. (2024). Identifikasi struktur geologi daerah panas bumi Way Panas Kecamatan Wonosobo menggunakan analisis FHD dan SVD berdasarkan data gaya berat GGMPlus. *5*(1). https://doi.org/10.29303/goescienceed.v5i1.240.
[43] Wibowo, R. C., & Tobing, J. B. L. (2022). Geological structure identification using derivative analysis of gravity method. *JIT: Journal of Innovation Technology, 3*(2). https://doi.org/10.31629/jit.v3i2.5048
[44] Ibrahim, D., Sumai, K., & Tengah, I. (2009). *Buku 1: Bidang energi* (pp. 273–294).
[45] Daud, Y., *et al*. (2019). Resistivity characterization of the Arjuno–Welirang volcanic geothermal system (Indonesia) through 3-D magnetotelluric inverse modeling. *Journal of Asian Earth Sciences, 174*, 352–363. https://doi.org/10.1016/j.jseaes.2019.01.033.
[46] Zhang, R. (2019). *Joint inversion of 2D gravity gradiometry and magnetotelluric data in mineral exploration*.